

# 2D Simulation of the Harmonic Motion Imaging (HMI) With Experimental Validation

Caroline Maleke, Jianwen Luo and Elisa E. Konofagou  
Department of Biomedical Engineering, Columbia University, New York, USA

**Abstract**— Amplitude-modulated (AM) harmonic motion imaging (HMI) is one of the radiation-force-based techniques, which has the capability of imaging tissue mechanical properties during the application of the acoustic radiation force. Since only displacement images have been presented until now, the theory between tissue displacement and modulus in AM-HMI has not been validated. Here, a finite-element model (FEM) is used to accurately model the dynamic response in tissue mimicking phantoms to evaluate HMI performance. The FEM and experimental results of phantoms with the same stiffness variations are compared and used to describe the behavior of tissue during the application of the stimulus. A harmonic force was generated by a 4.68 MHz single-element focused ultrasound (FUS) transducer. Since the focus is highly localized and has a harmonic response from AM beam, the motion characteristics can be directly related to the regional tissue modulus. The resulting motion was imaged simultaneously using a diagnostic (pulse-echo) transducer at center frequency of 7.5 MHz. RF signals were acquired using a standard pulse-echo technique with a PRF of 5.4 kHz. 1D cross-correlation technique was performed to estimate the resulting axial displacement. In the FEM simulation, a rectangular mesh with dimensions of 35 mm in the axial and 30 mm in the lateral directions was generated. There were a total of 2771 nodes and 5424 triangular elements in the mesh. For simplicity, the mesh was assumed to be a purely elastic medium with Young's modulus of 10 kPa. The acoustic pressure field was simulated in Field II using the same transducer parameters as in the experiment. This pressure field was used as the excitation force to generate displacements. The imaging field was simulated in Matlab 7.2 using a 2D convolutional image formation model with 128 acoustic elements, a center frequency of 7.5 MHz and 40 MHz sampling frequency. Only the displacement estimation at the center RF lines was considered in the validation with the single-element pulse-echo transducer used in the experiments. A good agreement between the results from the FEM and experiment findings was observed in phantom study. Finally, *in vivo* application is presented.

**Keywords:** Breast, Cancer, Displacement, FUS, Harmonic Motion Imaging, HIFU, In vivo, Noninvasive, Oscillatory, Radiation force, Tumor.

## I. INTRODUCTION

Acoustic radiation-force-based imaging methods have been studied by several research groups. These studies include acoustic radiation force impulse (ARFI) imaging [1], supersonic shear imaging [2], shear wave elasticity imaging (SWEI) [3], ultrasound stimulated acoustic emission (USAE) [4,5], and harmonic motion imaging (HMI) [6,7]. ARFI uses an impulse radiation force to induce brief mechanical excitations locally and image the resulting tissue response

while RF data are collected during tissue relaxation. USAE used two confocal ultrasound transducers to generate a localized oscillatory radiation force at low (kHz) frequency in tissues. The resulting tissue displacement produced a localized acoustic source that emitted an acoustic signal recorded by a hydrophone. The application of the acoustic radiation-force as a mechanical stimulus using an ultrasonic beam has been of particular interest in the last few years with applications in artery calcifications *in vitro* [4], *in vitro* porcine muscle [7], *in vitro* porcine liver [8] as well as *ex vivo* [9] and *in vivo* breast cancer [10].

HMI is a radiation-force technique that induces oscillatory displacements at the focus of the focused ultrasound (FUS) beam for the detection of localized stiffness changes [7]. When amplitude-modulation (AM) (25 Hz) is applied, the focus is stable within the tissue region [8]. This method offers the advantages of a simpler transducer design compared to two-transducers configuration [7]. The confocal transducer consists of a 4.68-MHz FUS and a 7.5-MHz diagnostic (pulse-echo) transducers is used [8]. Since both FUS and diagnostic beams are used simultaneously, the resulting oscillatory tissue motion can be monitored during oscillations.

Our aim was to map the tissue mechanical properties and map harder tumors mainly for breast, liver and prostate tissues. The FUS transducer was driven by a low acoustic power, but sufficient to induce adequate motion with an associated minute temperature rise. The radiation force was applied in a 2D fashion using a raster-scan technique. The 3D HMI image was obtained by combining multiple 2D planes at different depths. The AM-HMI technique has been successfully used to image breast tumor tissues *ex vivo*, e.g. benign and malignant [11], that include regions of higher stiffness. In this paper, we provided a finite-element model (FEM) validation of the AM-HMI technique as well as demonstrated the ability of this technique to identify the mammary tumor location in a mouse *in vivo*.

## II. METHODS

### Finite-Element Model

A rectangular mesh with a total of 2771 nodes and 5424 triangular elements was assembled. The tissue and inclusions were modeled as different material properties according to Table I. The mesh had dimensions of 35 mm in the axial and 30 mm in the lateral directions (Comsol Multiphysics<sup>TM</sup>, Comsol Inc., Burlington, MA, USA). For simplicity, the mesh was assumed to be a pure elastic medium with an assigned Poisson's ratio of 0.49 and a density of 1.0 g/cm<sup>3</sup>. The model

was assumed to be in a plane strain state and time dependent. Finer triangular elements allowed for accurate simulation of the spatial distribution and the consequent tissue response to acoustic pressure of the HMI technique. The acoustic intensity field was simulated in Field II [12] using the same FUS transducer parameters used in the experiment. The resulting intensity field was used as the excitation force to generate displacements. The acoustic intensity was normalized and scaled to a peak *in situ*, the peak average intensity value was  $236 \text{ W/cm}^2$  at a focal depth of 20 mm.

TABLE I. MESH MODELS

	Background stiffness (kPa)	Inclusion diameter (mm)	Inclusion stiffness (kPa)
Homogeneous	10	N/A	N/A
Type 1	10	4, 8 and 16	40
Type 2	10	4	20, 30, 40, and 50

The image formation model was simulated in Matlab 7.2 (Mathworks, Natick, MA, USA) using a 2D convolutional image formation model [13,14] with 128 acoustic elements, a center frequency of 7.5 MHz and a 40 MHz sampling frequency. Only the displacement estimation on the center RF line was considered in the validation with the single-element pulse-echo transducer used in experiments. A 1D cross-correlation technique on consecutive RF signals was used to estimate axial displacement with a window size equal of 0.47 mm and a 90% overlap.

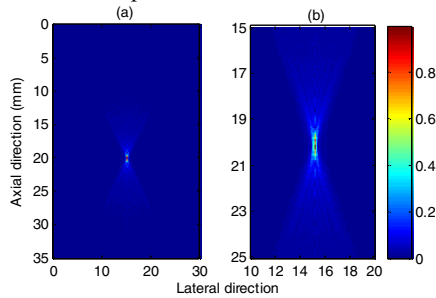


Fig. 1. The simulated distribution of acoustic pressure in the axial-lateral plane, focused at 20 mm. Transducer was centered at the top of the figure.

#### Experimental setup and data acquisition

The experimental setup is shown in Fig. 2. A 4.68 MHz FUS transducer (Riverside Research Institute, New York, NY, USA) was used to generate the acoustic radiation force using a low-frequency AM signal. A frequency generator (Agilent (HP) 33120A, Palo Alto, CA, USA) was used to produce RF signals at 4.68 MHz. The amplitude of the RF signals was then modulated using a second frequency generator (Agilent (HP) 33220A, Palo Alto, CA, USA) that generated a low frequency modulation at 25 Hz.

A pulse-echo transducer (Panametrics, Waltham, MA, USA) with a center frequency of 7.5 MHz and a diameter of 12 mm was placed through the void center of the FUS transducer, with the beams of the two transducers aligned. A

pulser/receiver (Panametrics 5051PR, Waltham, MA, USA) was used to drive the pulse-echo transducer at a PRF of 5.4 kHz. The RF signals were acquired using a standard pulse-echo technique. An analog bandpass filter (Reactel, Inc., Gaithersburg, Maryland, USA) with cutoff frequencies of  $f_{c1}=5.84\text{MHz}$  and  $f_{c2}=8.66\text{MHz}$  was used to filter the fundamental frequency of the therapy beam and its harmonics [8].

A water chamber containing degassed water was placed in between the FUS transducer and the anesthetized mouse as a beam propagation path. The mouse was placed in a supine position on a heating platform (THM100, Indus Instruments, Houston, TX, USA) to keep the mouse warm and comfortable. A silicone rubber/absorber (McMaster-Car, Dayton, NJ, USA) was placed beneath the mouse to further reduce the specular reflection from the heating platform. This platform was connected to an EKG device that allowed us to monitor the mouse heart rate.

The filtered RF signals were captured at 80 MHz at a 14-bit digitization rate (CS14200, Gage Applied Technologies, Lachine, Canada). M-mode frames were acquired during the raster-scanned process, and each M-mode frame contained 600 RF lines and had at least two periods of the AM oscillation. The time interval between two successive M-mode frames was approximately 0.73 s, i.e., the frame rate was equal to 1.2 frame/s.

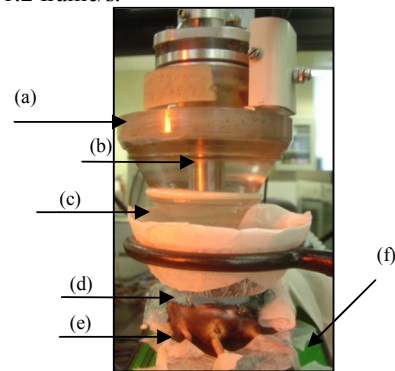


Fig. 2. Experimental setup. (a) FUS transducer, (b) pulse-echo transducer, (c) water chamber, (d) mouse, (e) an absorber, and (f) heating platform.

For HMI mapping, a harmonic radiation force was applied at each point in a 2D fashion using a raster-scan technique with a pulse AM of 10 cycles at duty cycle of 25% at intensity of  $231 \text{ W/cm}^2$ . The transducer was moved along a 2D grid with a step size of 1 mm using a computer-controlled positioner (Velmex Inc., Bloomfield, NY, USA). Multiple 2D planes at different depths were combined to generate a 3D HMI image.

### III. RESULTS

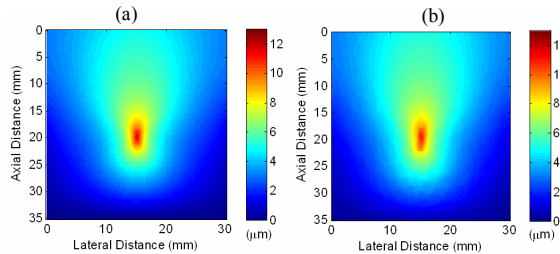
#### Finite-element Model

Figure 3 shows the cumulative displacement fields from mechanics model and HMI-estimated displacement in a homogenous medium with a Young's modulus of 10 kPa after HMI excitation. The displacement is localized and occurs

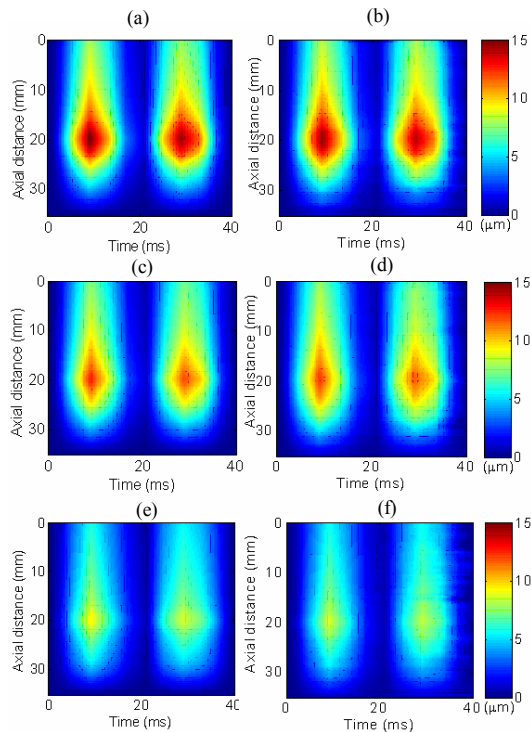
mainly at the focus of the transducer (at a depth of 20 mm), spanning approximately  $\pm 3$  mm laterally from the focal zone.

Figure 4 depicts the estimated HMI displacement (M-mode) for type I-mesh (Table I) from the FEM (a,c,e) and the simulated RF signal (HMI-estimated displacement) (b,d,f) described in the Methods section. In this figure, the blue and red colors represent the harmonic displacements moving away from and toward the transducer, respectively. The highest HMI displacements occur at the focus (Fig. 4). The frequency of the harmonic displacements is equal to the excitation frequency, i.e., 25 Hz.

Figure 5 illustrates quantitative results of displacement values along the central axis of the FUS transducer for homogeneous media (10kPa), Type-1 mesh for different 40 kPa-lesion sizes (4, 8, and 16 mm) and Type-2 mesh with a 4-mm-diameter inclusion for different stiffnesses (20, 30, 40, and 50 kPa).



**Fig. 3.** Cumulative displacement fields resulting from the acoustic force distribution (Fig. 1). The highest displacement occurs at a depth of 20 mm. (a) Mechanics model and (b) HMI estimated displacement.



**Fig. 4.** M-mode images of displacement from (a,c,e) FEM simulation and (b) HMI-estimated displacement for type I-mesh (Table I).

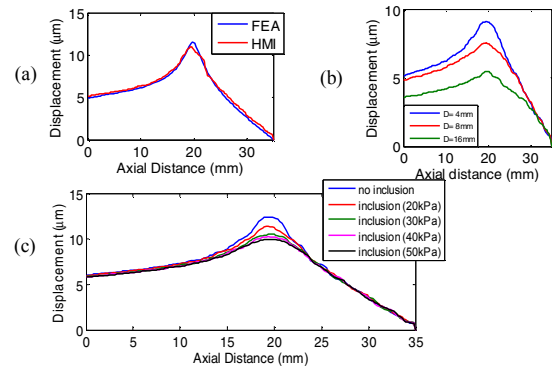


**Fig. 5.** Displacement values along the central axis of the FUS transducer for (a) homogeneous medium 10 kPa, (b) Type-1 mesh and (c) Type-2 mesh (Table I).

### Mechanical testing

A dynamic indentation test (Fig. 6) for acrylamide phantom gels [15] was conducted based on the Krouskop et al. [16] on an Instron Microtester (Instron, Inc., Norwood, MA) using a load cell rated to 10 N. The Instron machine had a computer interface that can be controlled to provide a displacement loading (Table II). The same gels were also tested using HMI technique. The mechanical testing (E vs. concentration) and HMI (1/displacement  $\sim E$ ) vs. concentration) profiles shared a similar linear trend along acrylamide concentration, where higher acrylamide concentration in the mixture produced a stiffer gel.

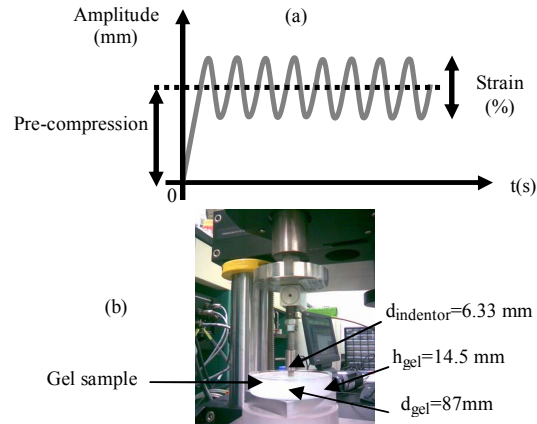


**Fig. 6.** (a) The applied pre-compression was 20% and 5% with dynamic loading or strain level of 5% and 2%, respectively for each gel. Both conditions were tested for loading frequencies of 0.1 Hz and 1 Hz. (b) Dynamic indentation test setup. (d=diameter)

TABLE II. MECHANICAL TESTING RESULTS

Acrylamide Concentration (%)	20% pre-compression (5% dynamic loading)		5% pre-compression (2% dynamic loading)	
	0.1 Hz	1Hz	0.1 Hz	1Hz
	Young's Modulus (Pa)			
25	13262	13363	13882	13162
30	24152	29091	24700	24156
35	36218	37111	37373	38835
40	49874	48400	51380	51375

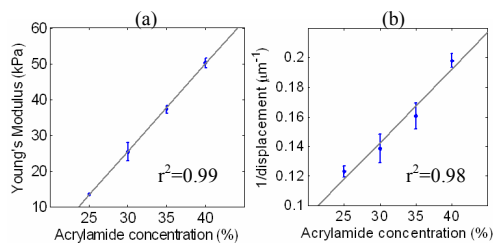


**Fig. 7.** (a) Mechanical testing and (b) HMI experimental results for gels at different acrylamide concentrations.

#### *In vivo* HMI mapping

Since AM beam creates a harmonic displacements as described in the method section, physiologic motion artifacts (i.e., from respiratory motion) can be identified, separated and successfully filtered and measured. Such an example is shown in Fig. 8 that was obtained during *in vivo* mapping of a human mammary planted in a tumor-mouse [17] where the respiration (Fig. 8b) was successfully removed. The resulting 2D-HMI displacements for axial, lateral and elevational planes are shown in Fig. 9.

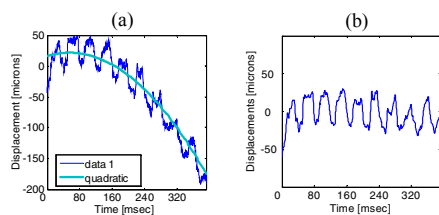


**Fig. 8.** (a) HMI measurement (with quadratic fitting) before and (b) after removal of respiration motion.

#### IV. CONCLUSION

The aim of this work is to investigate the potential of the amplitude-modulated (AM) harmonic motion imaging (HMI) technique for tumor mapping. FEM simulation shows that AM-HMI produces a localized harmonic displacement at the focal zone of the transducer. Two types of mesh are used to understand the sensitivity of the HMI technique for different lesion sizes and stiffnesses. The FEM results indicate that larger lesion sizes change the displacement profile due to the fact that the lesion will compress or stretch the background medium, because the effect of viscosity is not taken into consideration. In addition, HMI-estimated displacement and the Young's modulus show a linear trend, and thus indicate that HMI is a sensitive technique to assess different tissue stiffnesses. The *in vivo* result presented herein is to demonstrate that HMI is could map abnormal tissues, such as breast tumors, and identified physiologic motion artifacts (respiratory motion). This artifact is successfully separated and filtered. Further studies will involve FEM simulations that

will include important parameters (e.g., absorption and attenuation coefficients, and viscosity) as well as quantitative *in vivo* results.

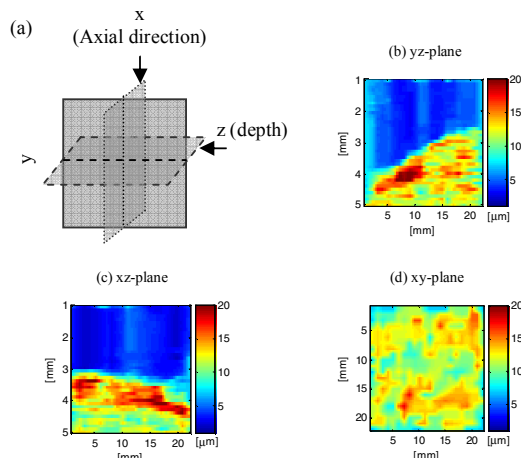


**Fig. 9.** Orthogonal HMI displacement images of the tumor in degassed water (blue or null displacement); (b) axial, (c) elevational and (d) lateral directions based on coordinate planes in (a).

#### ACKNOWLEDGMENT

This study was supported by a Special Development Award from the Whitaker Foundation and startup funds from Columbia University. The authors also wish to thank Wei-Ning Lee, MS and Viktor Gamarnik for valuable discussions, and the Riverside Research Institute (RRI) for providing the transducers used for this study.

#### REFERENCES

- [1] K. R. Nightingale et al., *J Acoust Soc Am*, 110, 625-34, 2001.
- [2] J. Bercoff et al., *IEEE Trans. Ultrason Ferroelectr Freq Control*, 51, 396-409, 2004.
- [3] A. P. Sarvazyan et al., *Ultrasound Med Biol*, 24, 1419-35, 1998.
- [4] M. Fatemi and J.F. Greenleaf, *Science*, 280, 82-85, 1998.
- [5] M. Fatemi and J.F. Greenleaf, *Physics Med Biol*, 45, 1449-1464, 2000.
- [6] E. Konofagou et al., *Physics Med Biol*, 46, 2967-2984, 2001.
- [7] E. E. Konofagou and K. Hynynen, *Ultrasound Med Biol*, 29, 1405-1413, 2003.
- [8] C. Maleke et al., *Ultrasonic Imaging*, 28, 144-158, 2006.
- [9] A. Alizad et al., *IEEE Trans Med Imaging*, 23, 307-312, 2004.
- [10] A. Alizad et al., *Ultrasonics*, 44, 1:e217-20, 2006.
- [11] C. Maleke et al., *International Congress on Ultrasonics*, Vienna, April 9 - 13, 2007.
- [12] J. A. Jensen and N. B. Svendsen, *IEEE Trans Ultrason Ferroelectr Freq Control*, 39, 262-267, 1992.
- [13] J. C. Bamber and R. J. Dickinson, *Phys Med Biol*, 25, 463-479, 1980.
- [14] D. A. Seggie et al., *IEEE Ultrasonics Symposium*, 714-717, 1983.
- [15] C. Lafon et al., *IEEE Ultrasonics Symposium*, 1295-1298 2001.
- [16] T. A. Krouskop et al., *Ultrasonic Imaging*, 20, 260-274, 1998.
- [17] T. Ludwig et al., *Genes & Devel.* 11: 1226-1241, 1997.